Chemosensing of Neurotransmitters with Selectivity and Naked Eye Detection of L-DOPA Based on Fluorescent Zn(II)-Terpyridine Bearing Boronic Acid Complexes

Iván J. Bazany-Rodríguez,[a] María K. Salomón-Flores,[a] Alejandro O. Viviano-Posadas,[a] Marco A. García-Eleno,[b] Joaquín Barroso-Flores[c*] Diego Martínez-Otero,[c] and Alejandro Dorazco-González [a*]

[a]*Instituto de Química, Universidad Nacional Autónoma de México, Circuito Exterior, Ciudad Universitaria, México, 04510, D.F., México.*
[b]*Centro Conjunto de Investigación en Química Sustentable, UAEM-UNAM, Carretera Toluca-Atlacomulco Km 14.5, C. P. 50200, Toluca, Estado de México, México. Facultad de Química, Universidad Autónoma del Estado de México.*
[c]*Centro Conjunto de Investigación en Química Sustentable, UAEM-UNAM, Carretera Toluca-Atlacomulco Km 14.5, C. P. 50200, Toluca, Estado de México, México. Instituto de Química, Universidad Nacional Autónoma de México*.
Corresponding author: E-mail: adg@unam.mx

Electronic Supporting Information

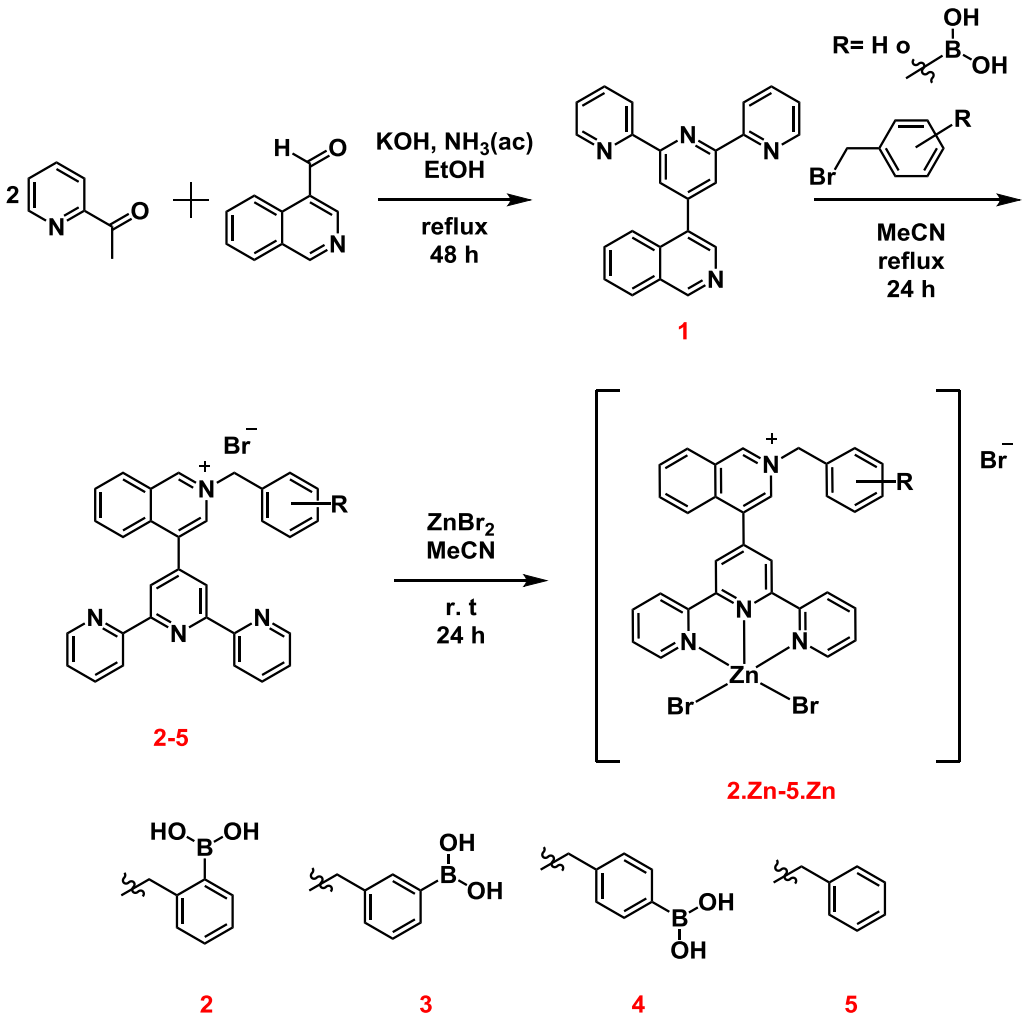

Table S1 Crystallographic data for **4.Zn** and **5.Zn.**

Crystal data[a]	**4.Zn**	**5.Zn**
Formula	$C_{31}H_{23.81}B_{0.81}Br_3N_4O_{1.63}Zn$	$C_{33}H_{29}Br_5N_4OSZn_2$
MW (g mol^{-1})	792.27	1059.95
Temperature (K)	100(2)	100(2)
Crystal system	Monoclinic	Monoclinic
Space group	$P2_1/c$	$P2_1/n$
a (Å)	14.9965(3)	11.8967(3)
b (Å)	13.1054(2)	13.6816(3)
c (Å)	17.7644(3)	22.4595(5)
α (°).	90°	90°
β (°)	109.7882(7)°	98.2926(10)°.
γ (°)	γ = 90°	90°
V(Å^3)	3285.17(10)	3617.42(15)
Z	4	4
P_{calcd} (g cm^{-3})	1.602	1.946
μ (mm-^{1})	5.566	8.905
R [I>2σ(I)][b]	0.0747	0.0446
R_w[d]	0.2299	0.1175

[a] $\lambda_{CuK\alpha}$ = 1.54178 Å; [b] F_o>4σ(F_o). [c] $R = \Sigma\|\underline{F_o}|-|F_c\|/\Sigma|F_o|$ [d] all data.

Table S2. Hydrogen bonds for **4.Zn** [Å and °].

D-H...A	d(D-H)	d(H...A)	d(D...A)	<(DHA)
O(1)-H(1)...Br(3)	0.84	2.61	3.269(8)	136.7
O(2)-H(2A)...Br(3)	0.84	2.45	3.230(8)	153.9

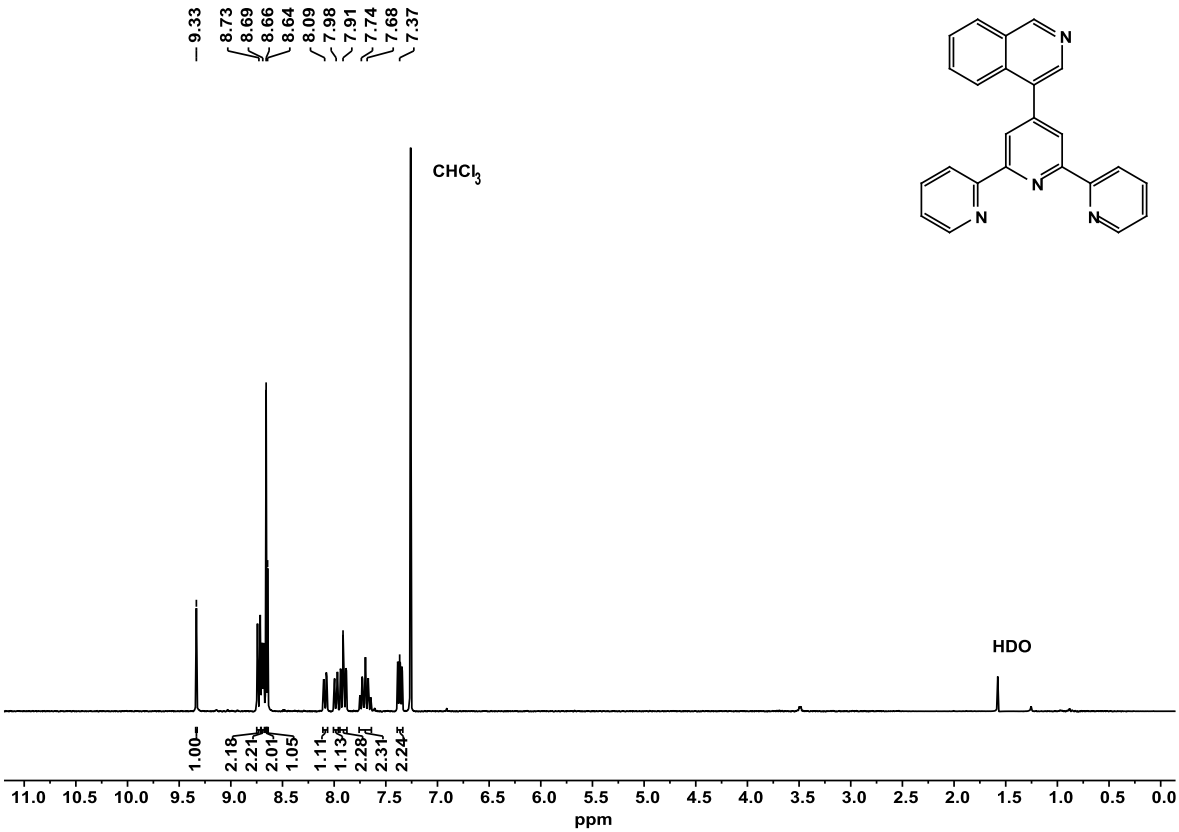

Fig. S1 ^{1}H NMR spectrum of **1** in $CDCl_3$.

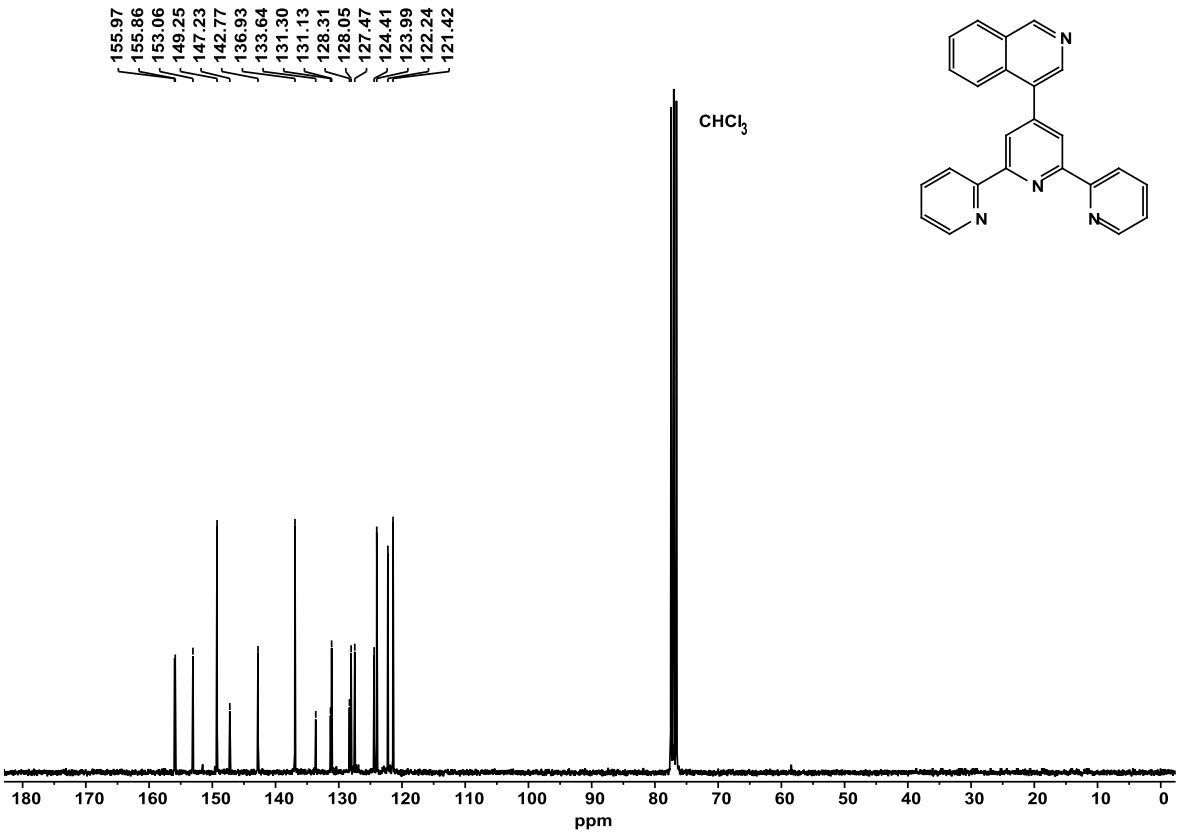

Fig. S2 ^{13}C NMR spectrum of **1** in $CDCl_3$.

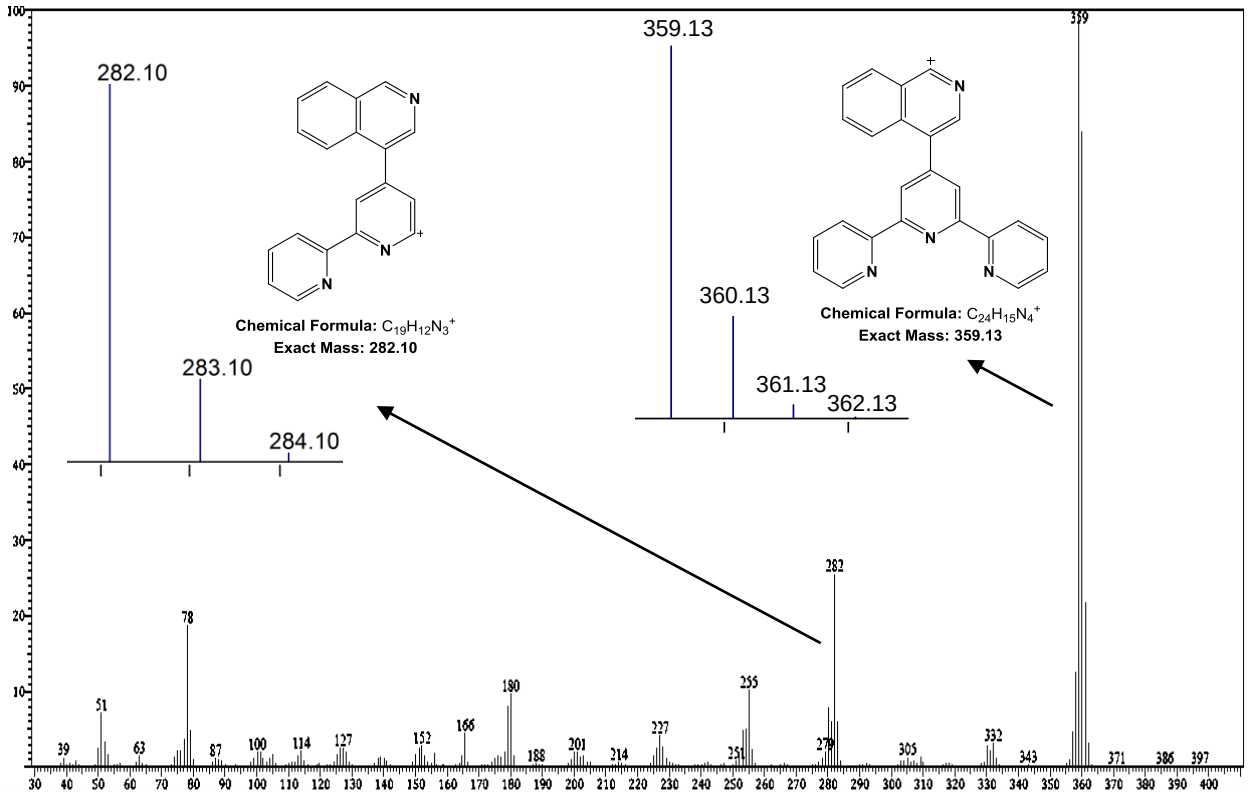

Fig. S3 Positive scan MS-EI spectrum of **1**. Inset: theoretically calculated MS isotopic patterns.

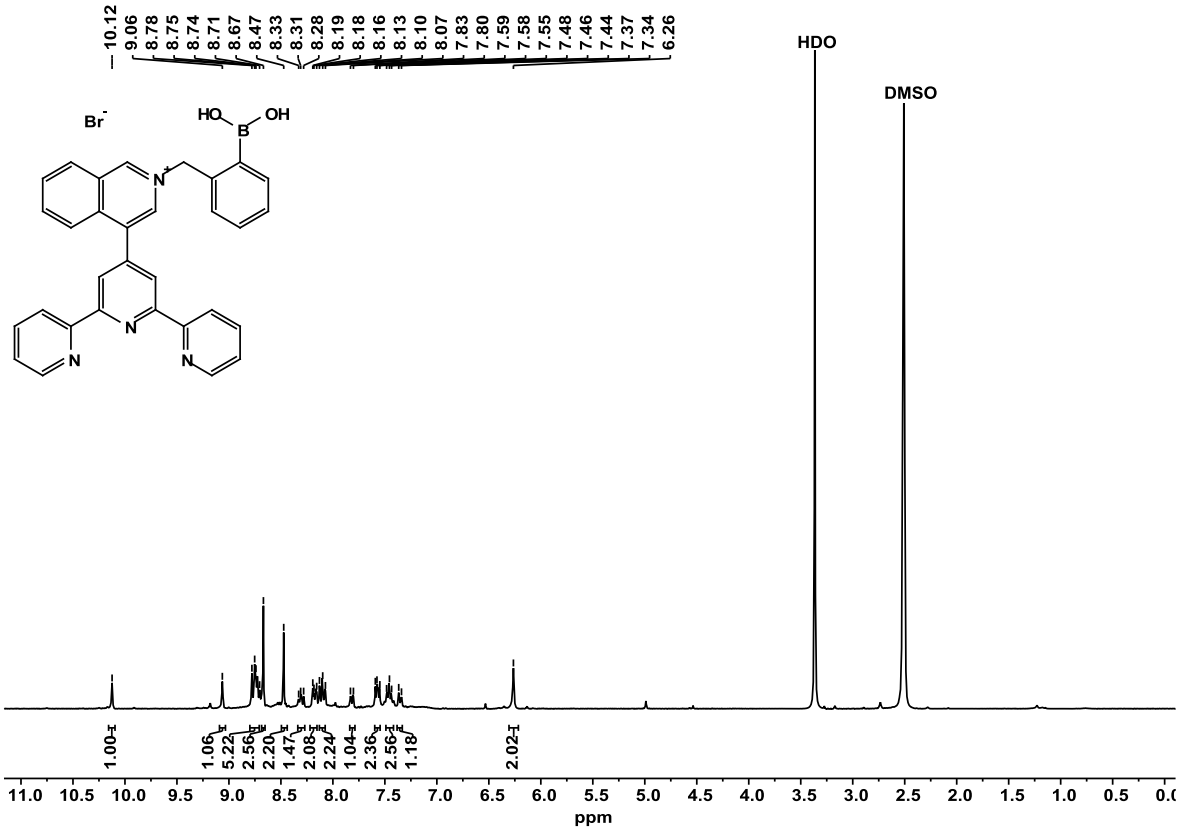

Fig. S4 ^{1}H NMR spectrum of **2** in DMSO-d_6.

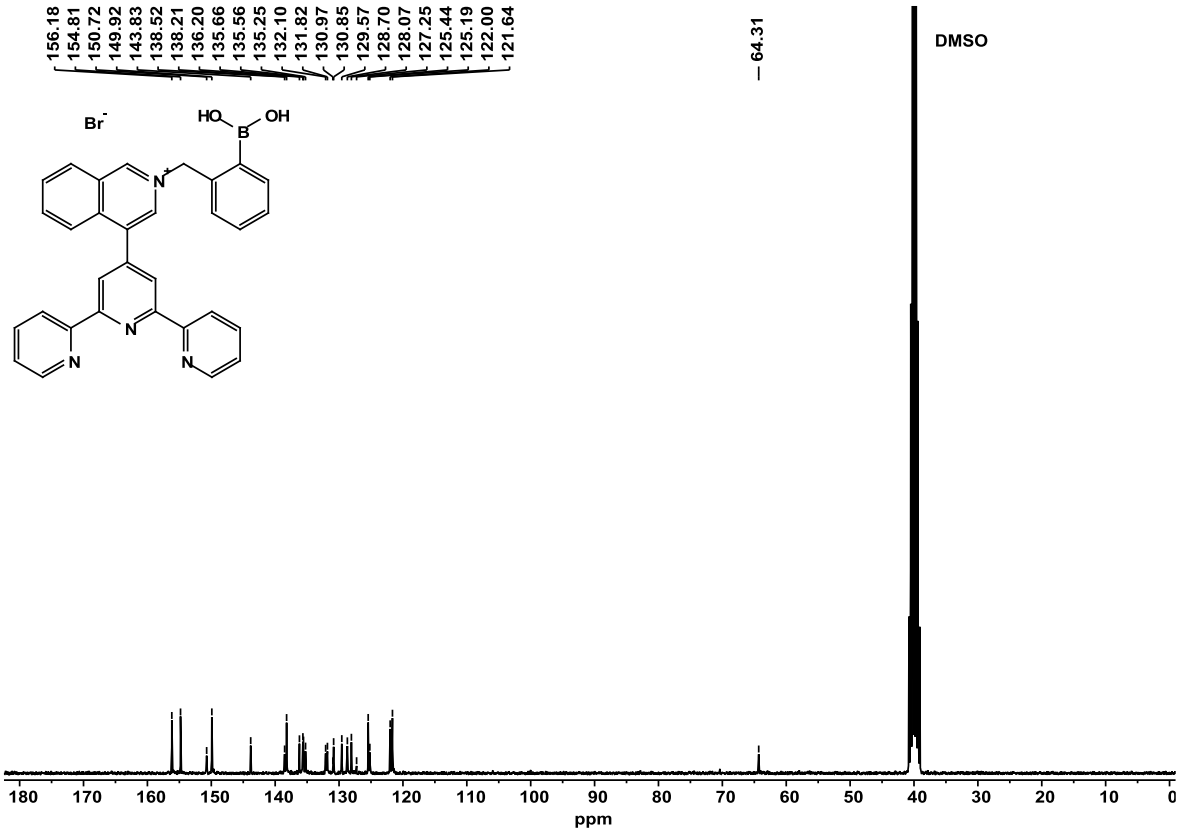

Fig. S5 ^{13}C NMR spectrum of **2** in DMSO-d_6.

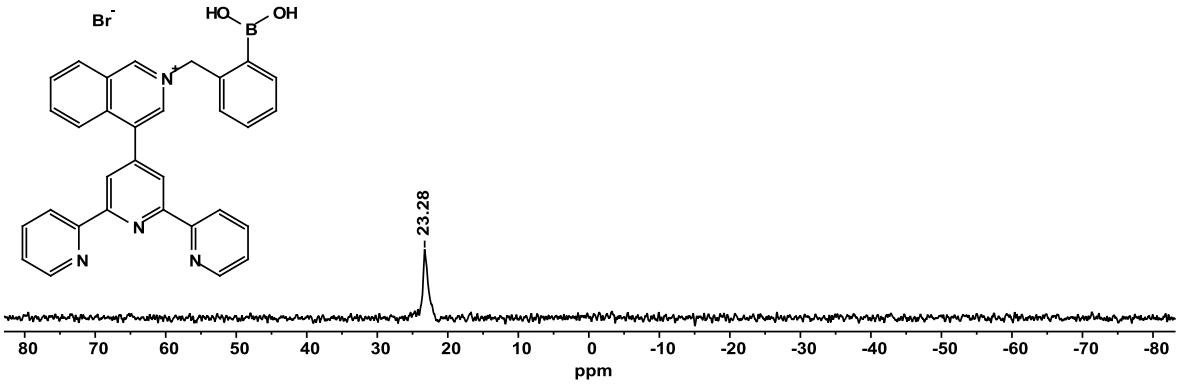

Fig. S6 ^{11}B NMR spectrum of **2** in DMSO-d_6.

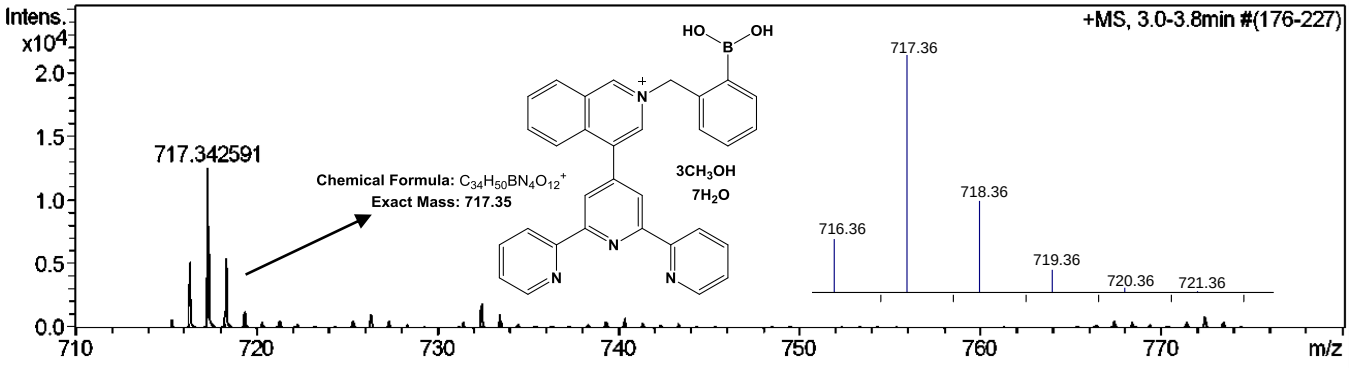

Fig. S7 Positive scan MS-ESI spectrum of **2**. Inset: theoretically calculated MS isotopic patterns.

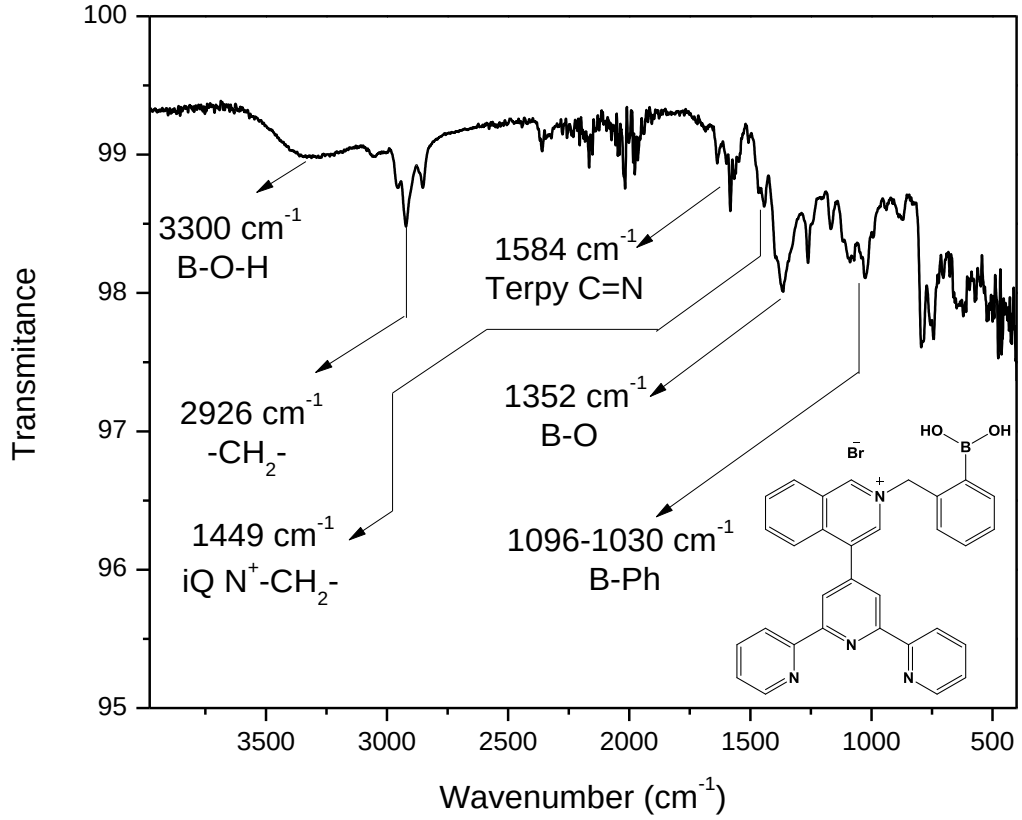

Fig. S8 IR (ATR) spectrum of **2**.

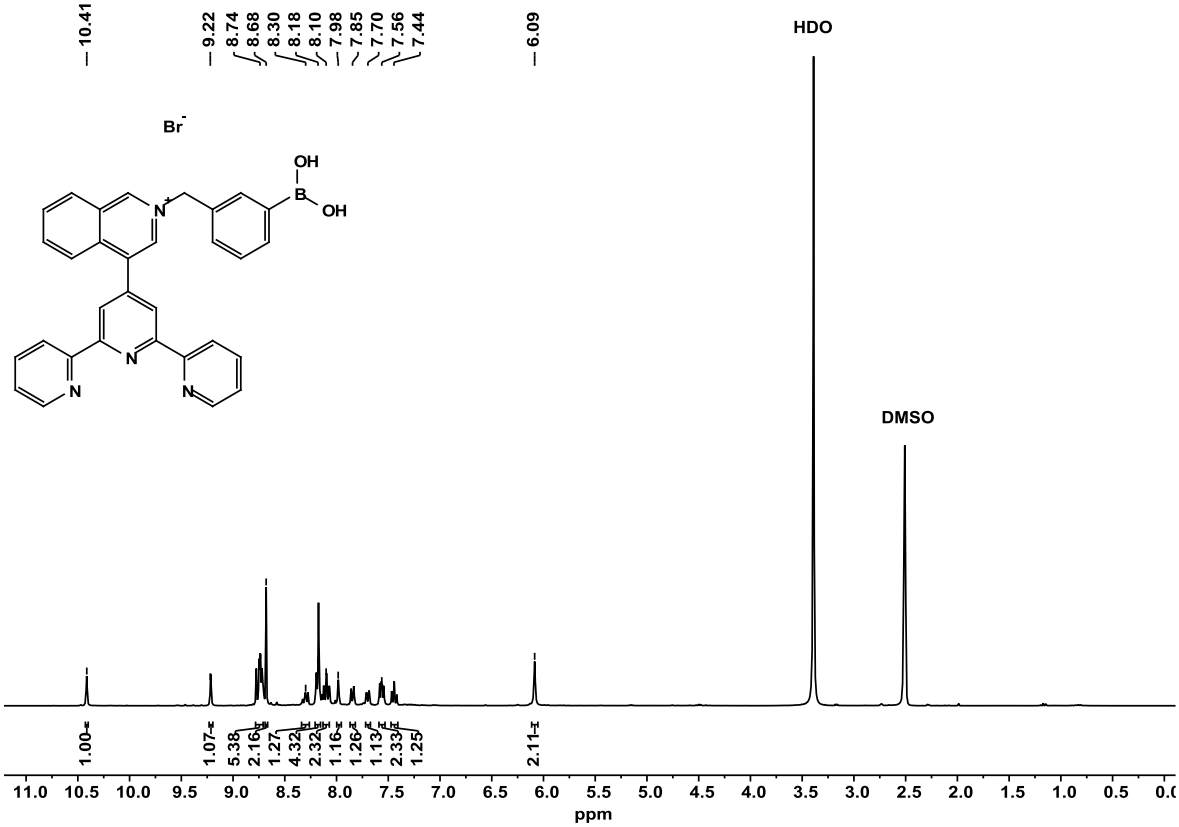

Fig. S9 ^{1}H NMR spectrum of **3** in DMSO-d_6.

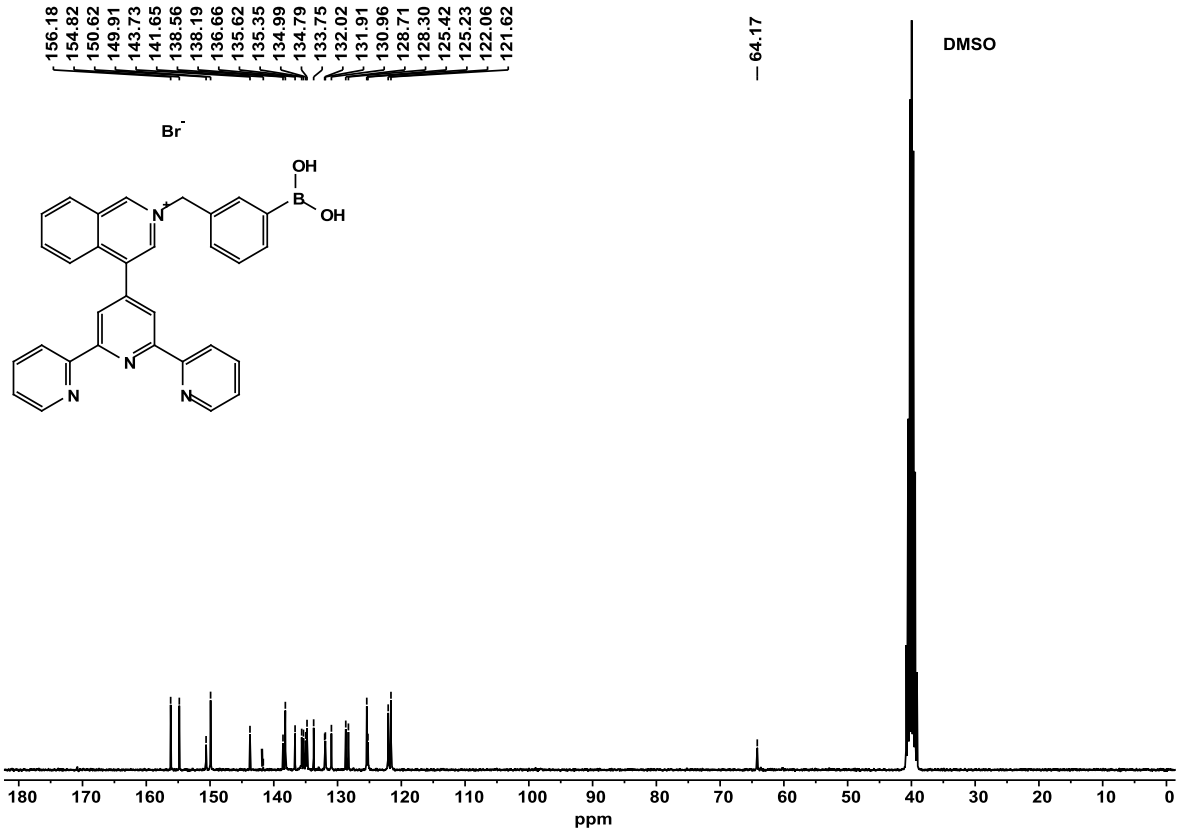

Fig. S10 ^{13}C NMR spectrum of **3** in DMSO-d_6.

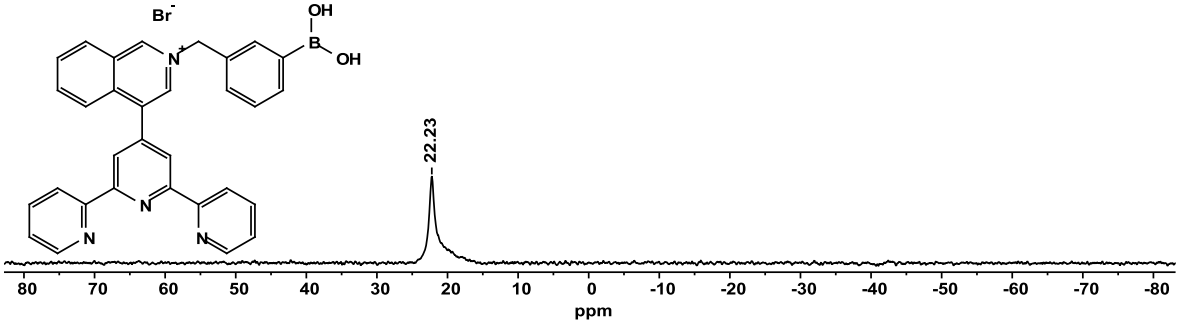

Fig. S11 ^{11}B NMR spectrum of **3** in DMSO-d_6.

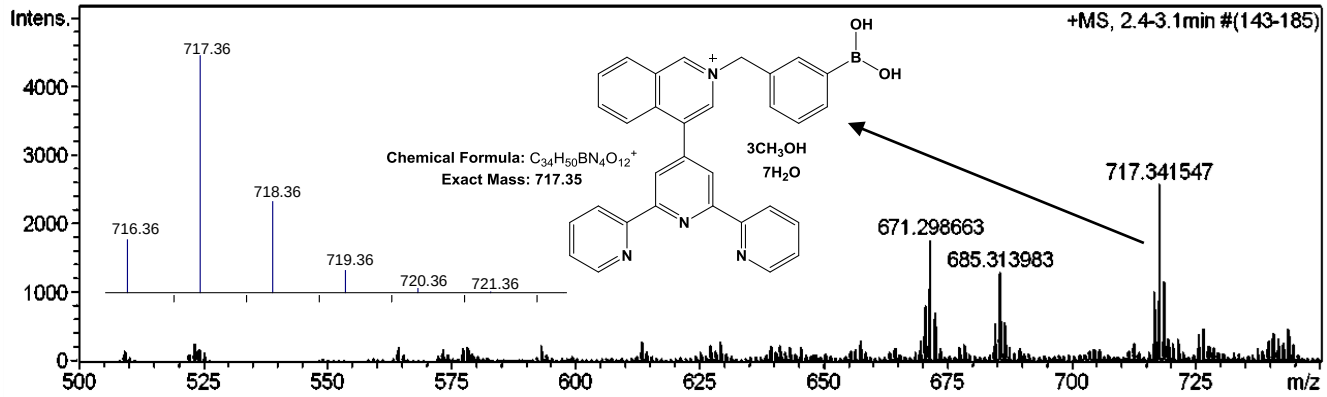

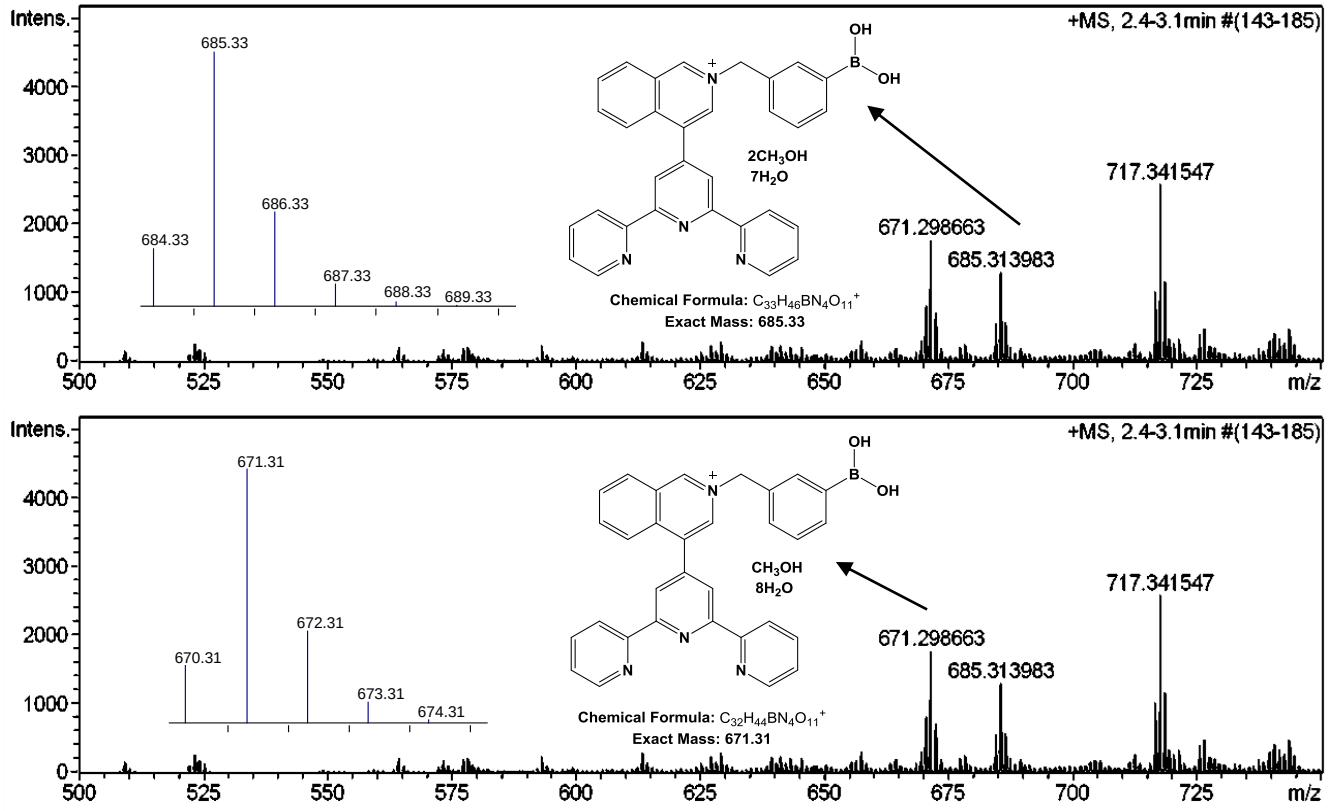

Fig. S12 Positive scan MS-ESI spectrum of **3**. Inset: theoretically calculated MS isotopic patterns.

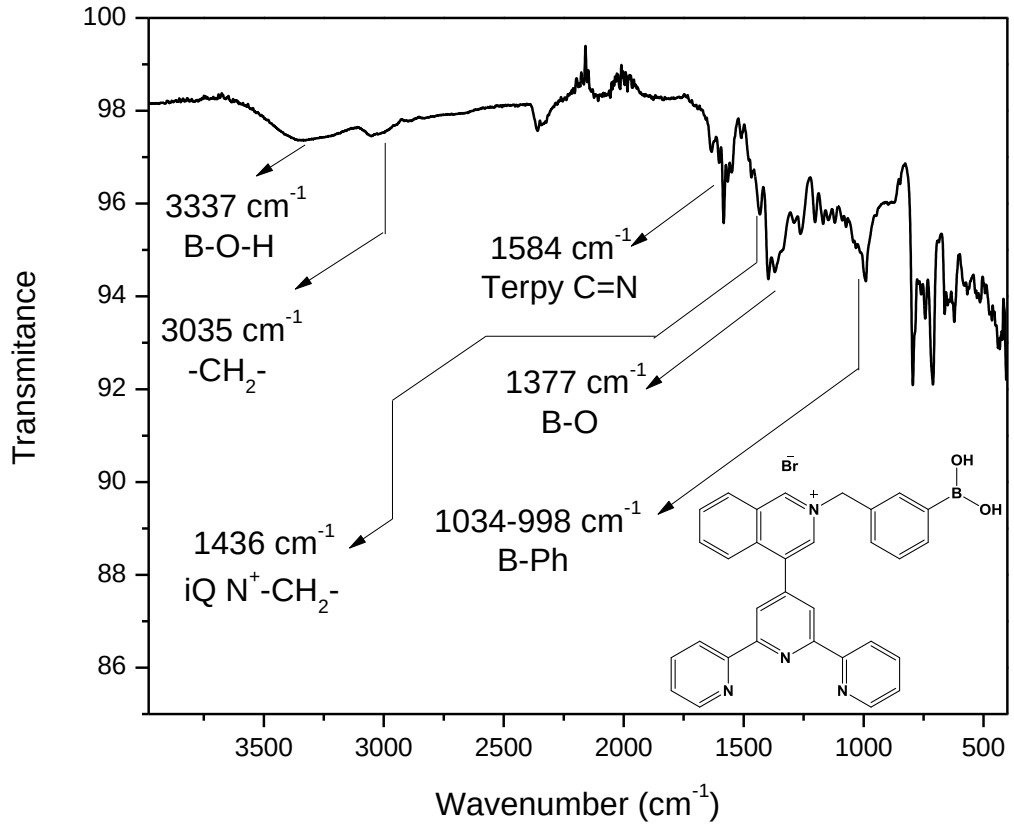

Fig. S13 IR (ATR) spectrum of **3**.

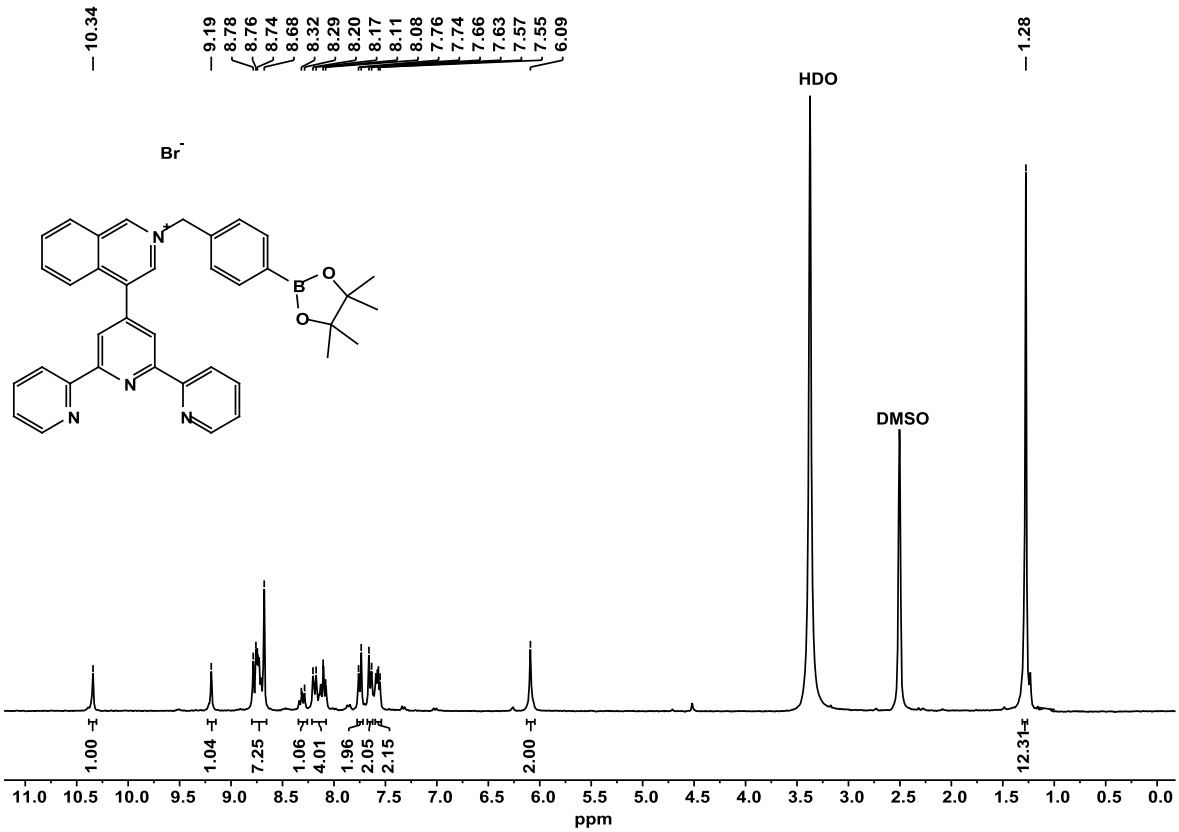

Fig. S14 ^{1}H NMR spectrum of **4** in DMSO-d_6.

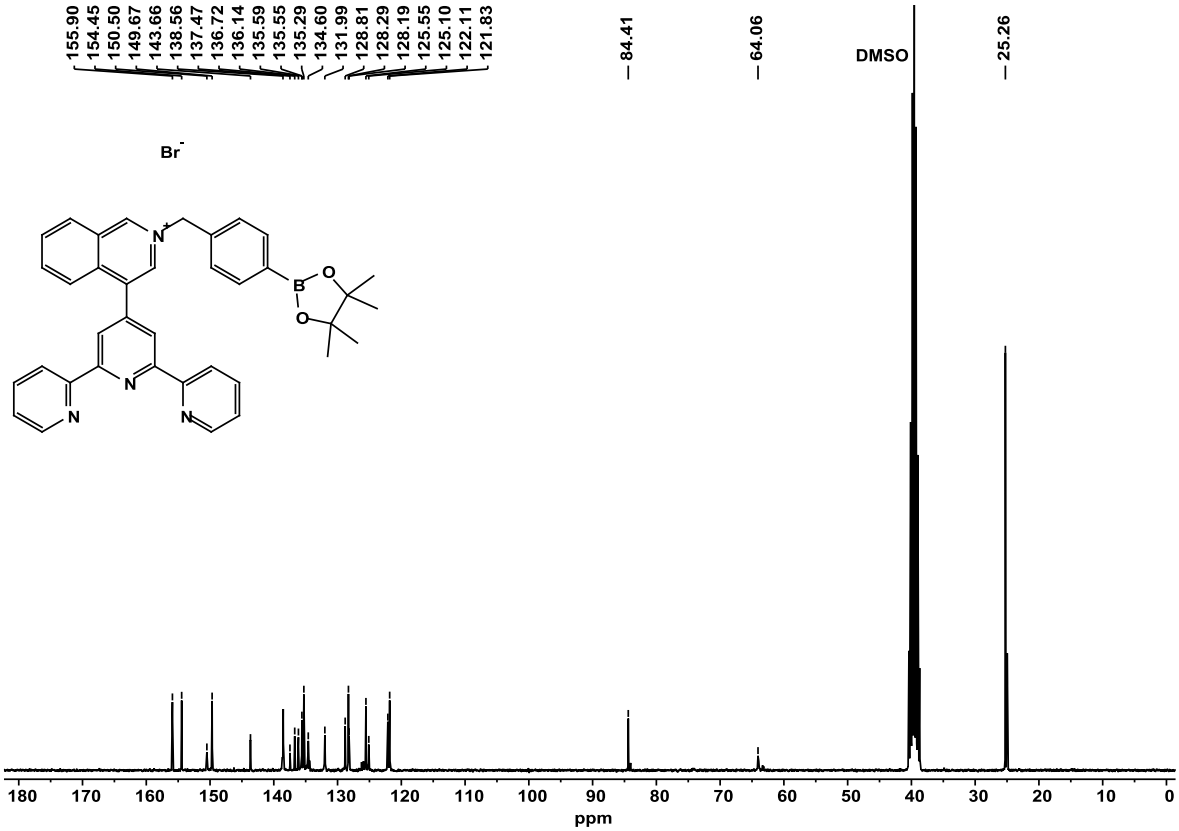

Fig. S15 ^{13}C NMR spectrum of **4** in DMSO-d_6.

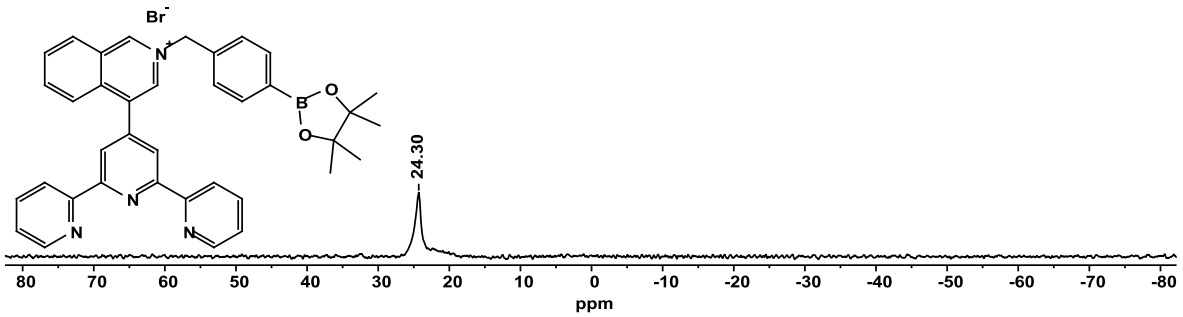

Fig. S16 ^{11}B NMR spectrum of **4** in DMSO-d_6.

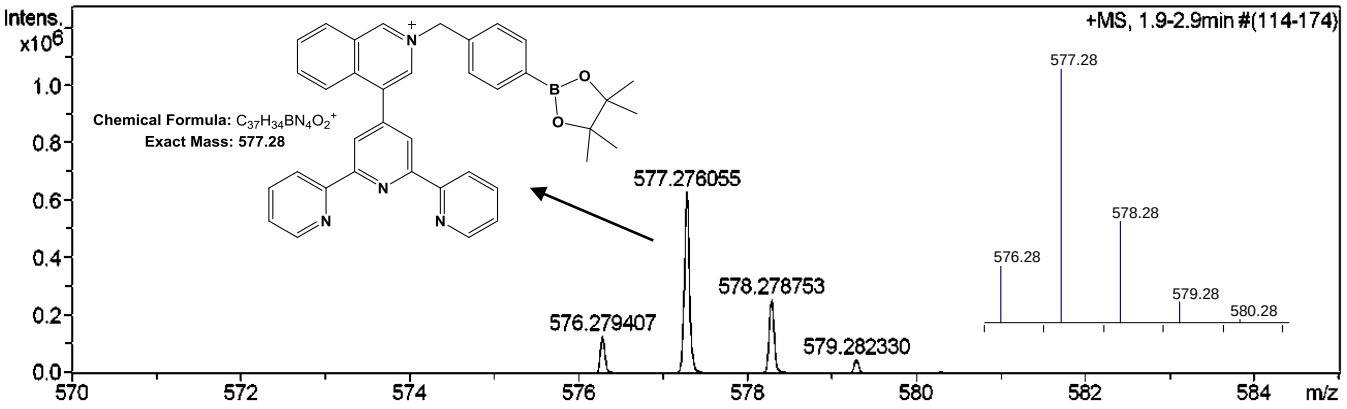

Fig. S17 Positive scan MS-ESI spectrum of **4**. Inset: theoretically calculated MS isotopic patterns.

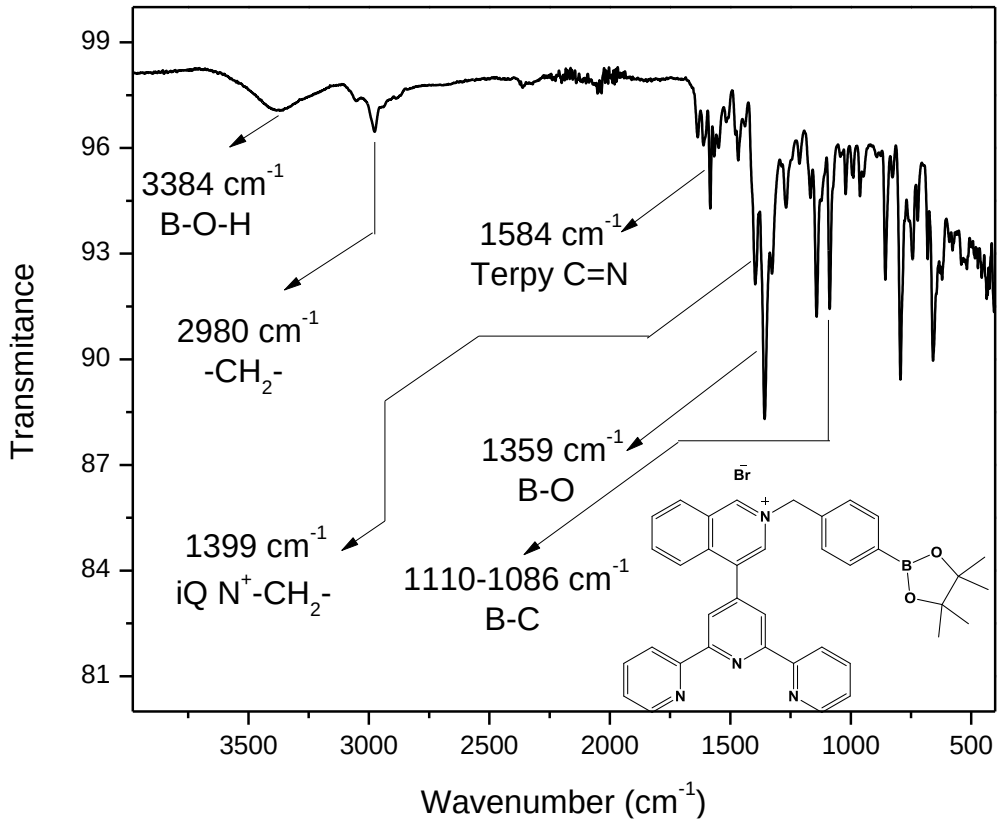

Fig. S18 IR (ATR) spectrum of **4**.

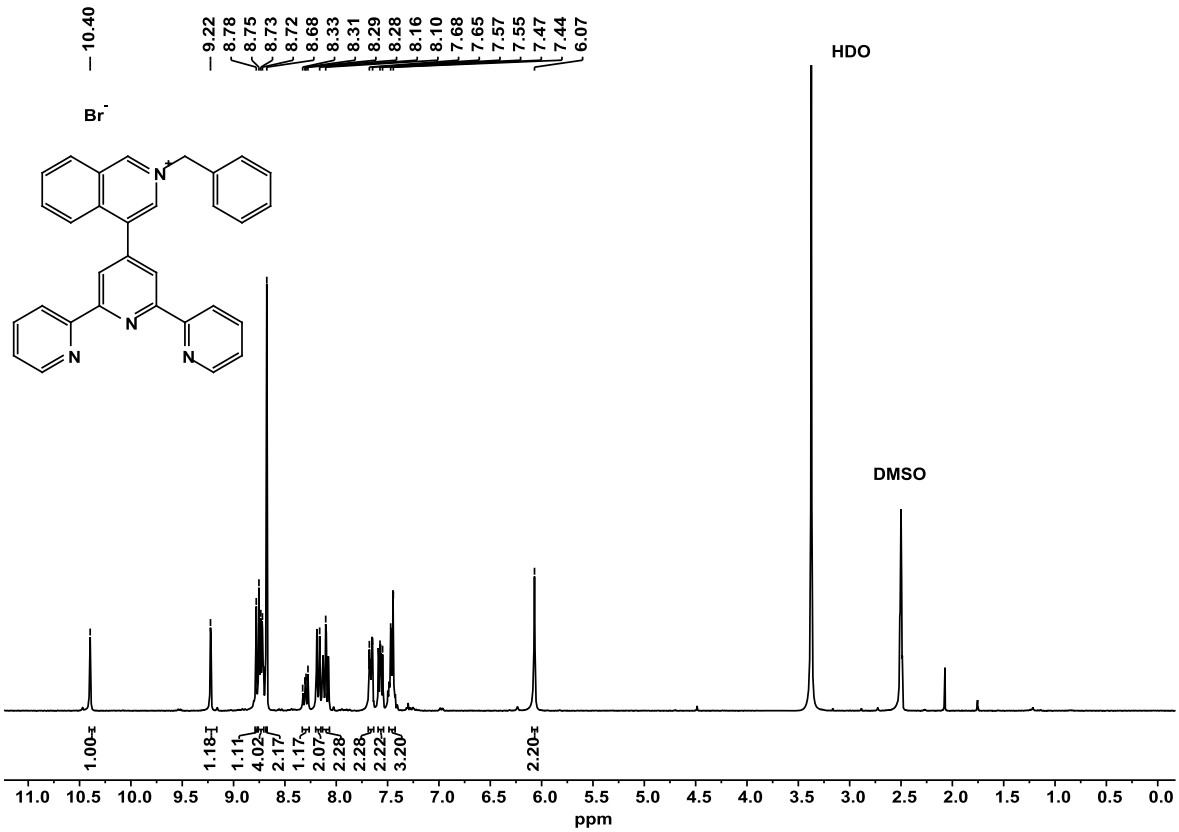

Fig. S19 ^{1}H NMR spectrum of **5** in DMSO-d_6.

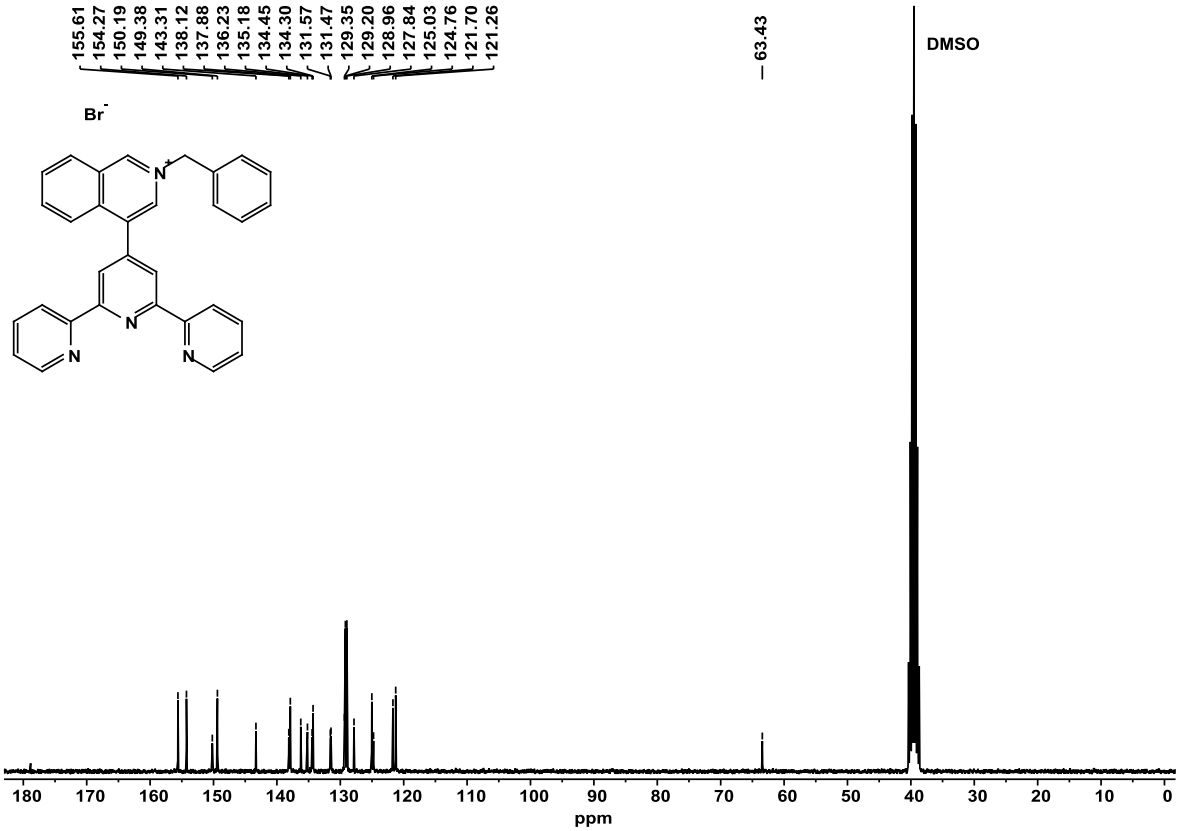

Fig. S20 ^{13}C NMR spectrum of **5** in DMSO-d_6.

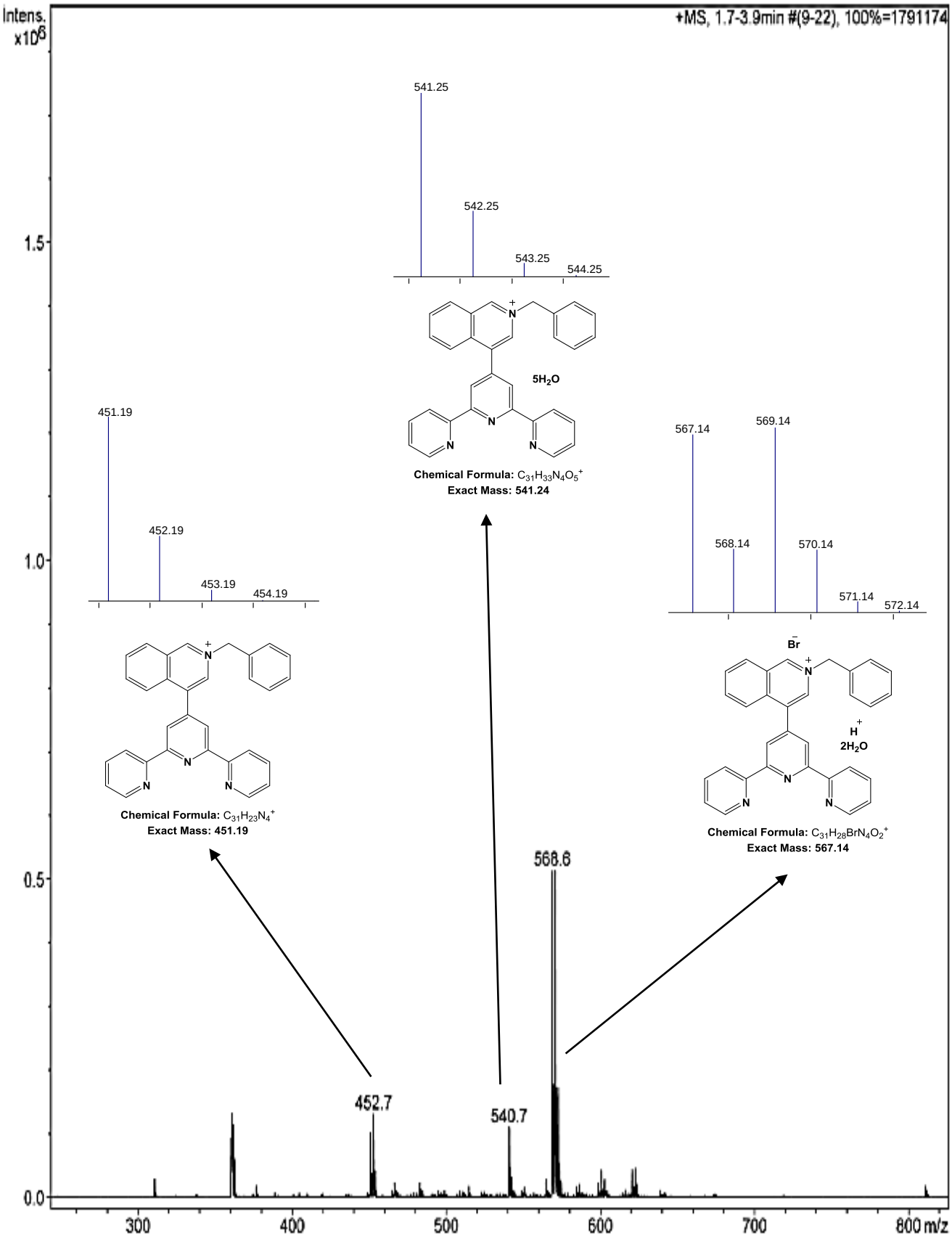

Fig. S21 Positive scan MS-APCI spectrum of **5**. Inset: theoretically calculated MS isotopic patterns.

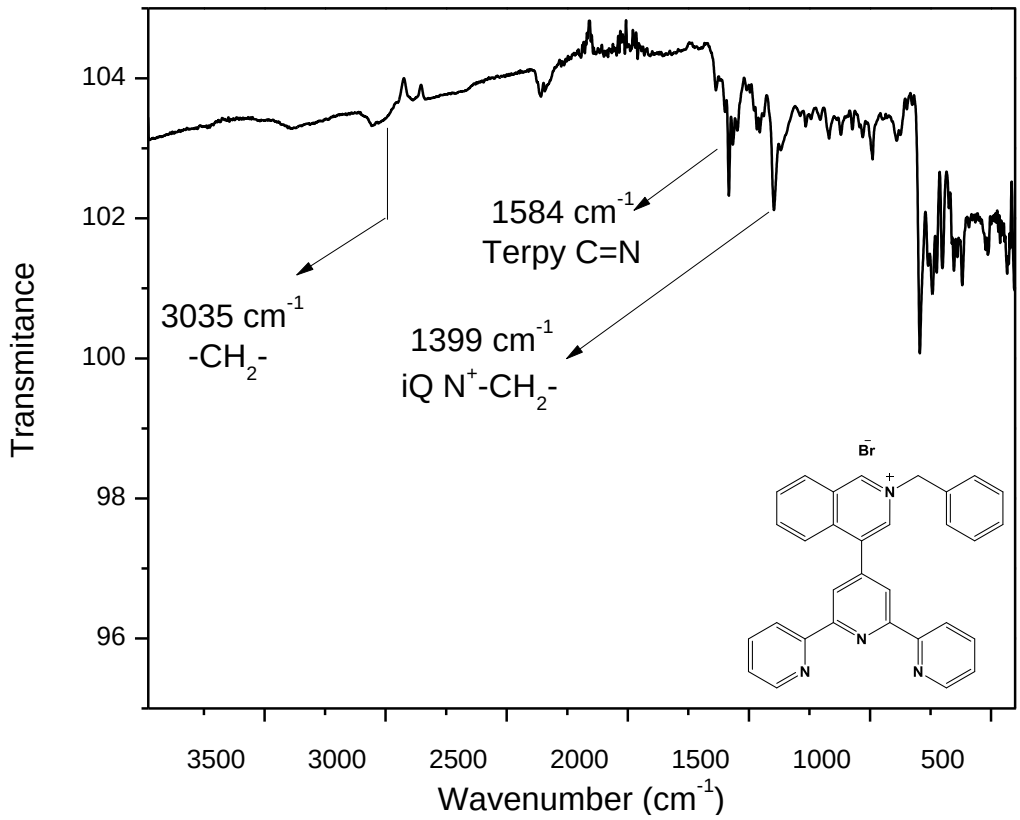

Fig. S22 IR (ATR) spectrum of **5**.

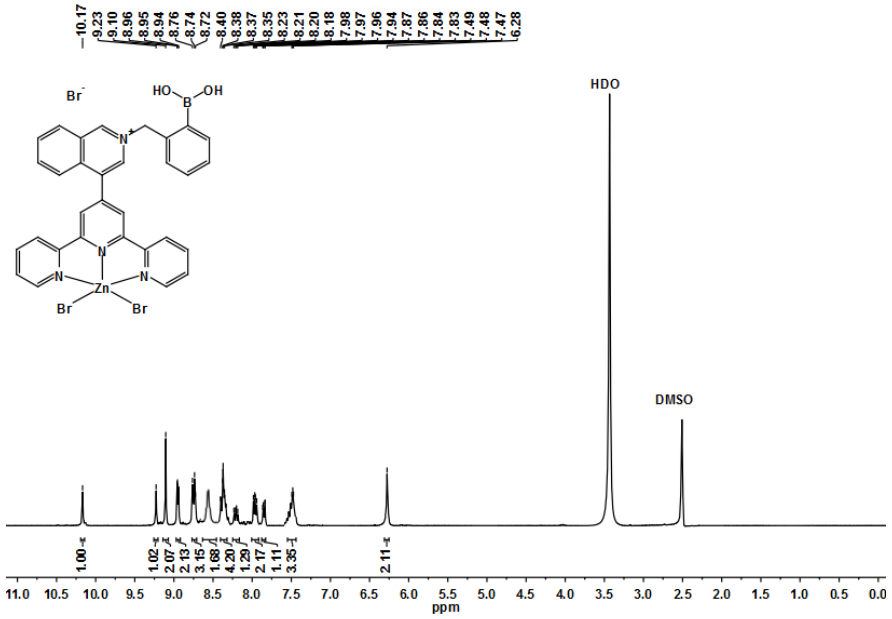

Fig. S23 ^{1}H NMR spectrum of **2.Zn** in DMSO-d_6.

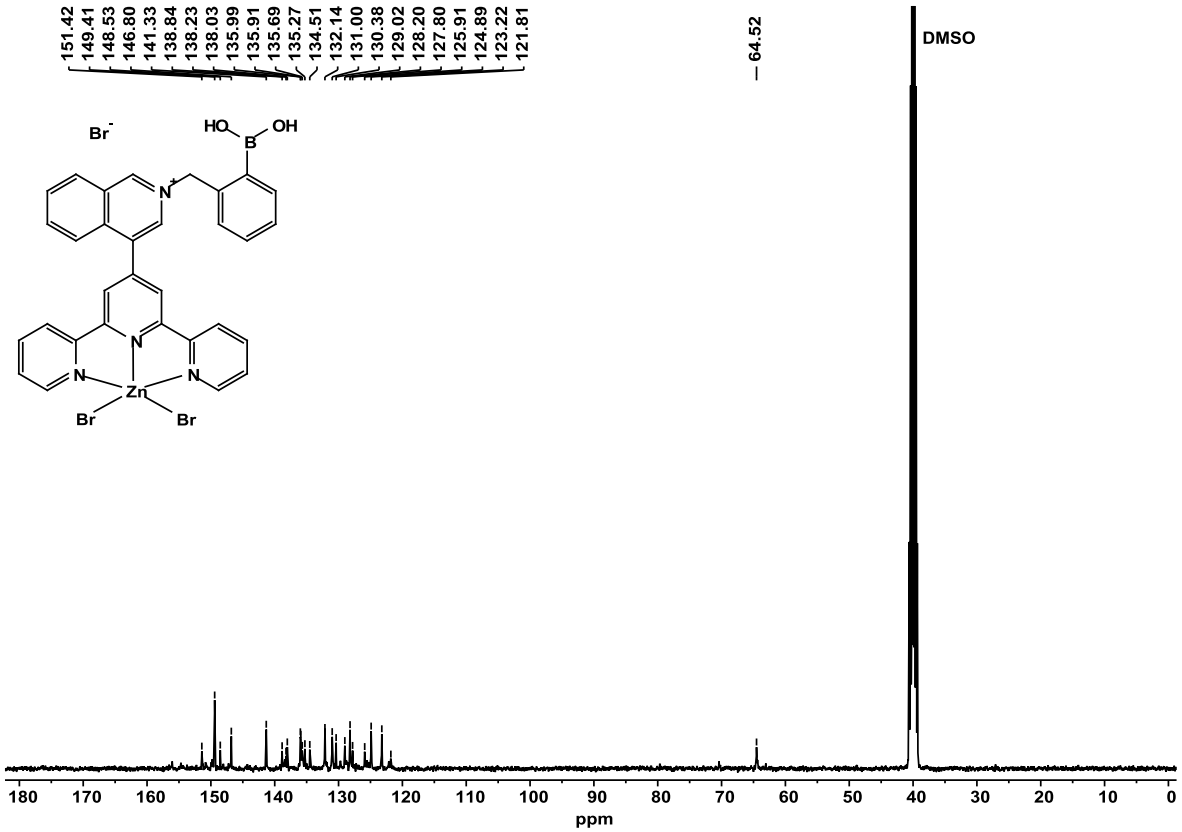

Fig. S24 ^{13}C NMR spectrum of **2.Zn** in DMSO-d_6.

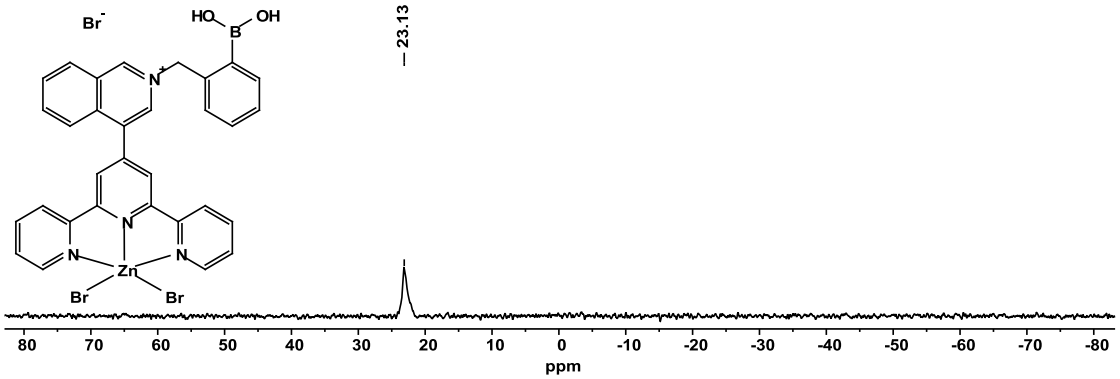

Fig. S25 ^{11}B NMR spectrum of **2.Zn** in DMSO-d_6.

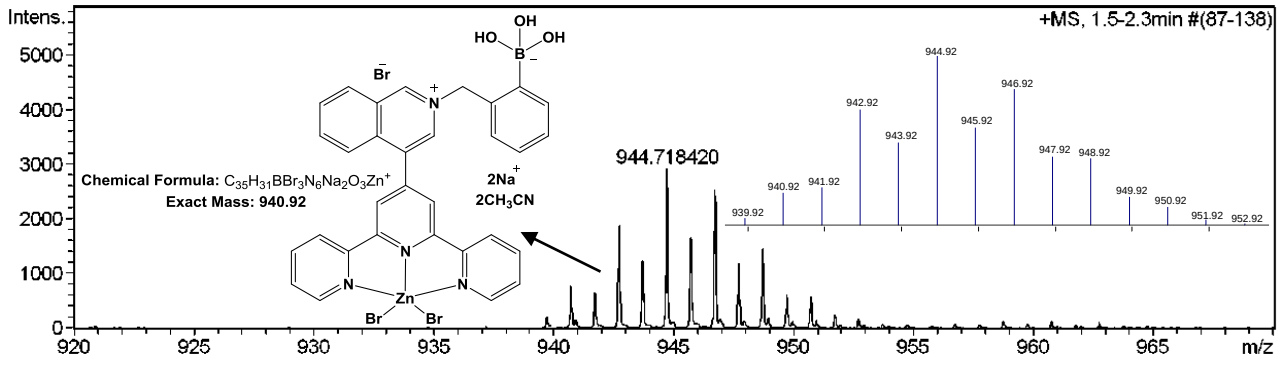

Fig. S26 Positive scan MS-ESI spectrum of **2.Zn**. Inset: theoretically calculated MS isotopic patterns.

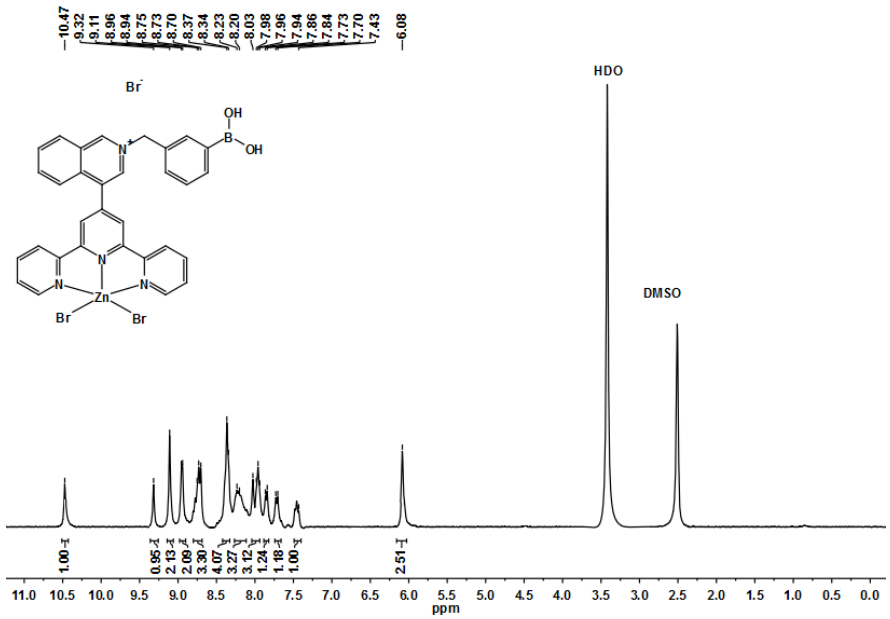

Fig. S27 ^{1}H NMR spectrum of **3.Zn** in DMSO-d_6.

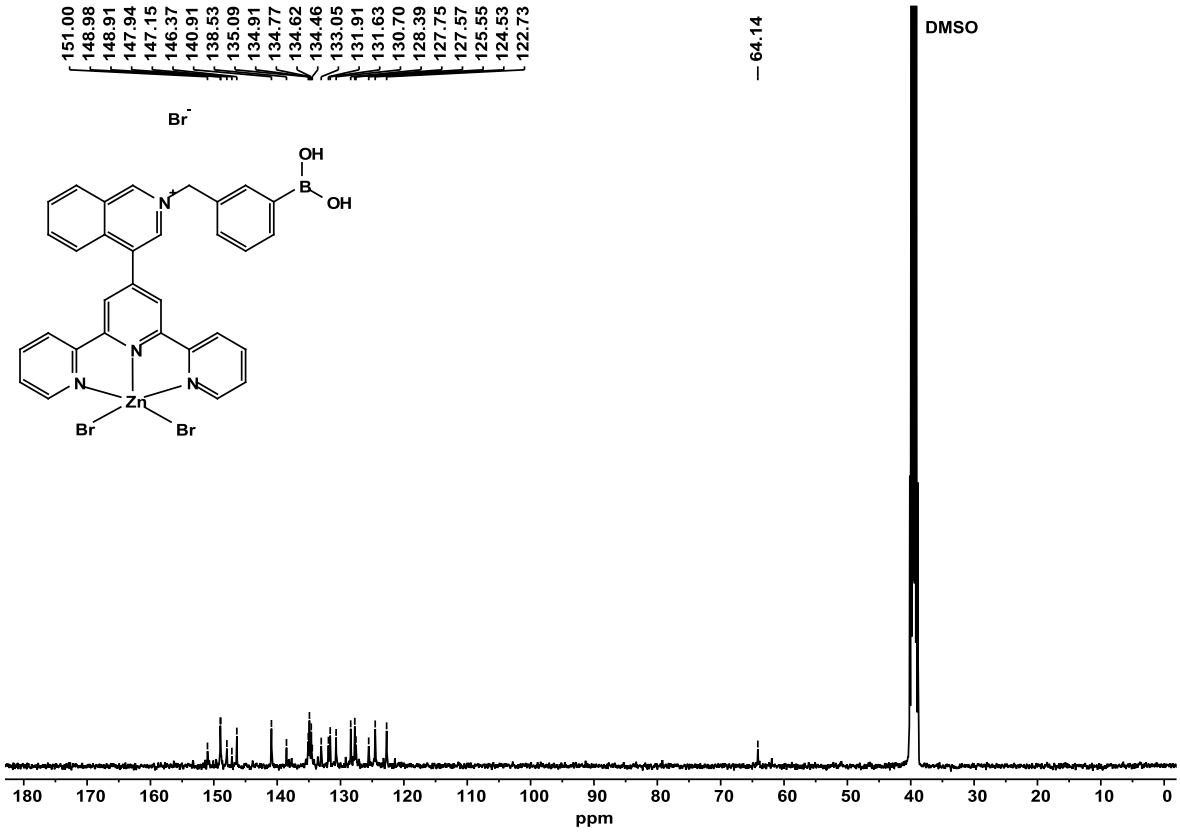

Fig. S28 ^{13}C NMR spectrum of **3.Zn** in DMSO-d_6.

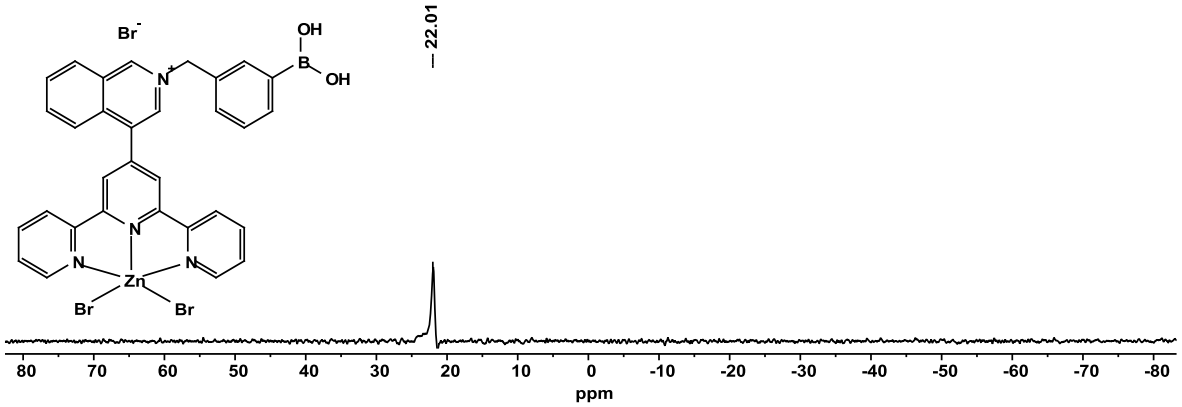

Fig. S29 ^{11}B NMR spectrum of **3.Zn** in DMSO-d_6.

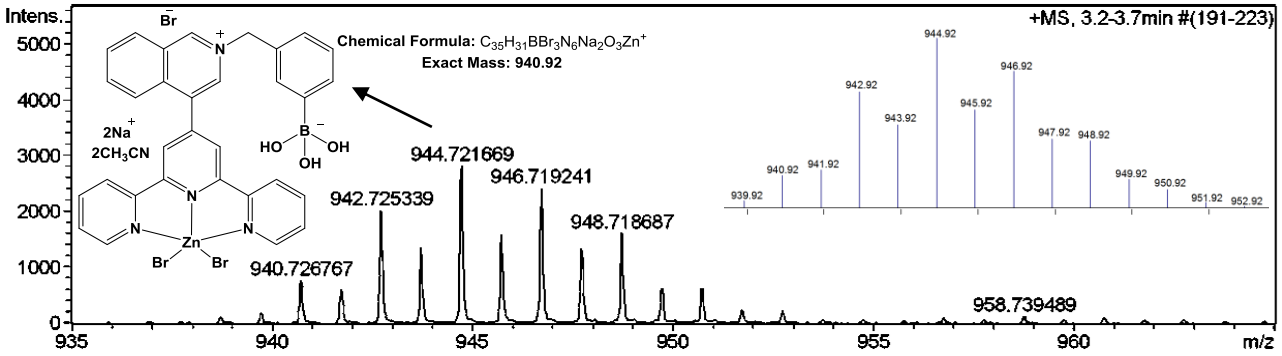

Fig. S30 Positive scan MS-ESI spectrum of **3.Zn**. Inset: theoretically calculated MS isotopic patterns.

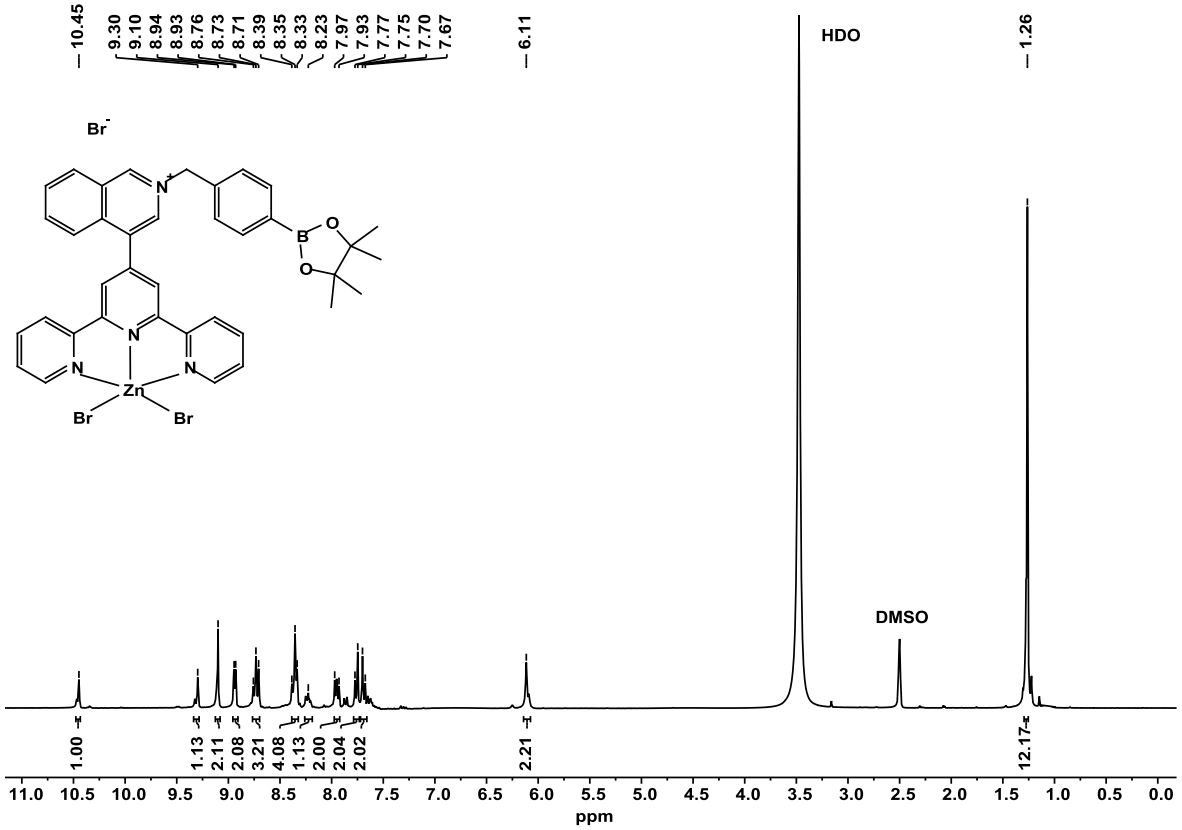

Fig. S31 ^{1}H NMR spectrum of **4.Zn** in DMSO-d_6.

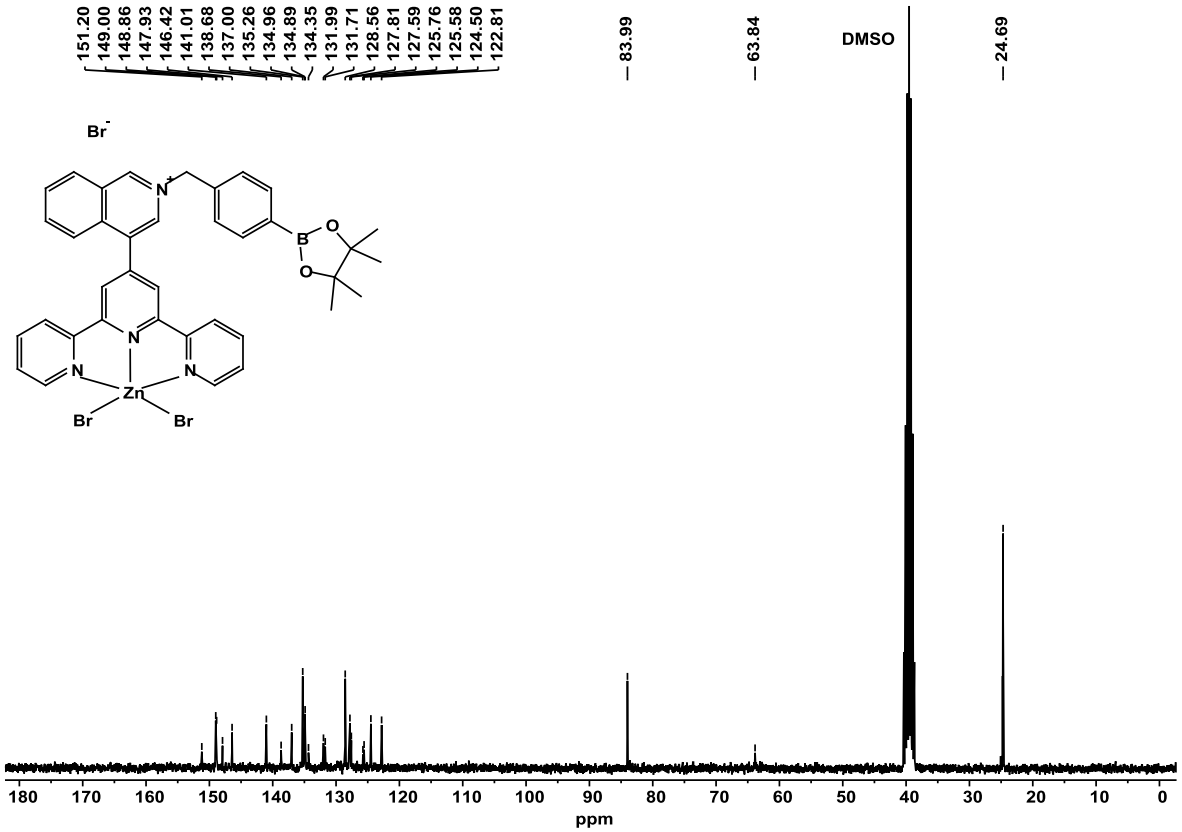

Fig. S32 ^{13}C NMR spectrum of **4.Zn** in DMSO-d_6.

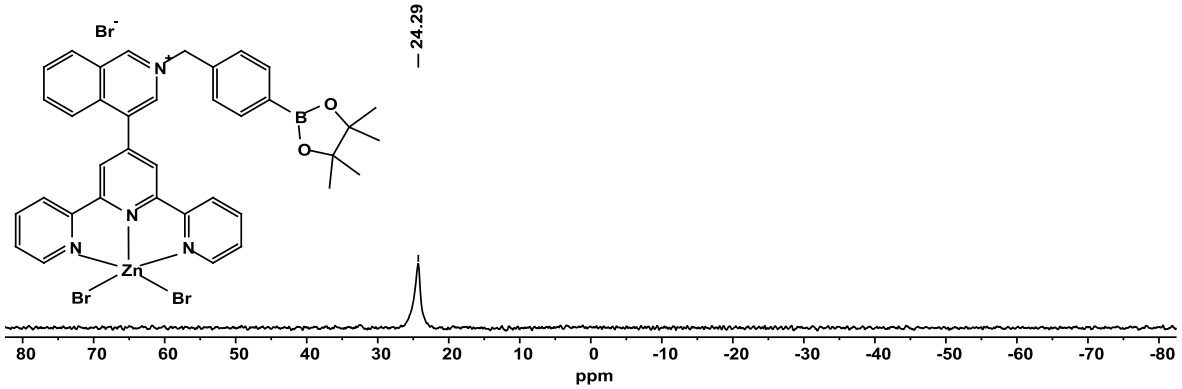

Fig. S33 ^{11}B NMR spectrum of **4.Zn** in DMSO-d_6.

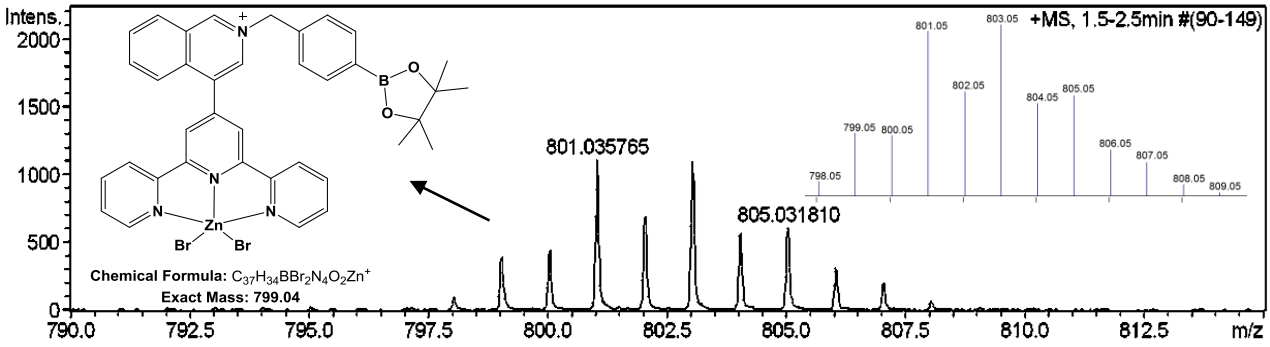

Fig. S34 Positive scan MS-ESI spectrum of **4.Zn**. Inset: theoretically calculated MS isotopic patterns.

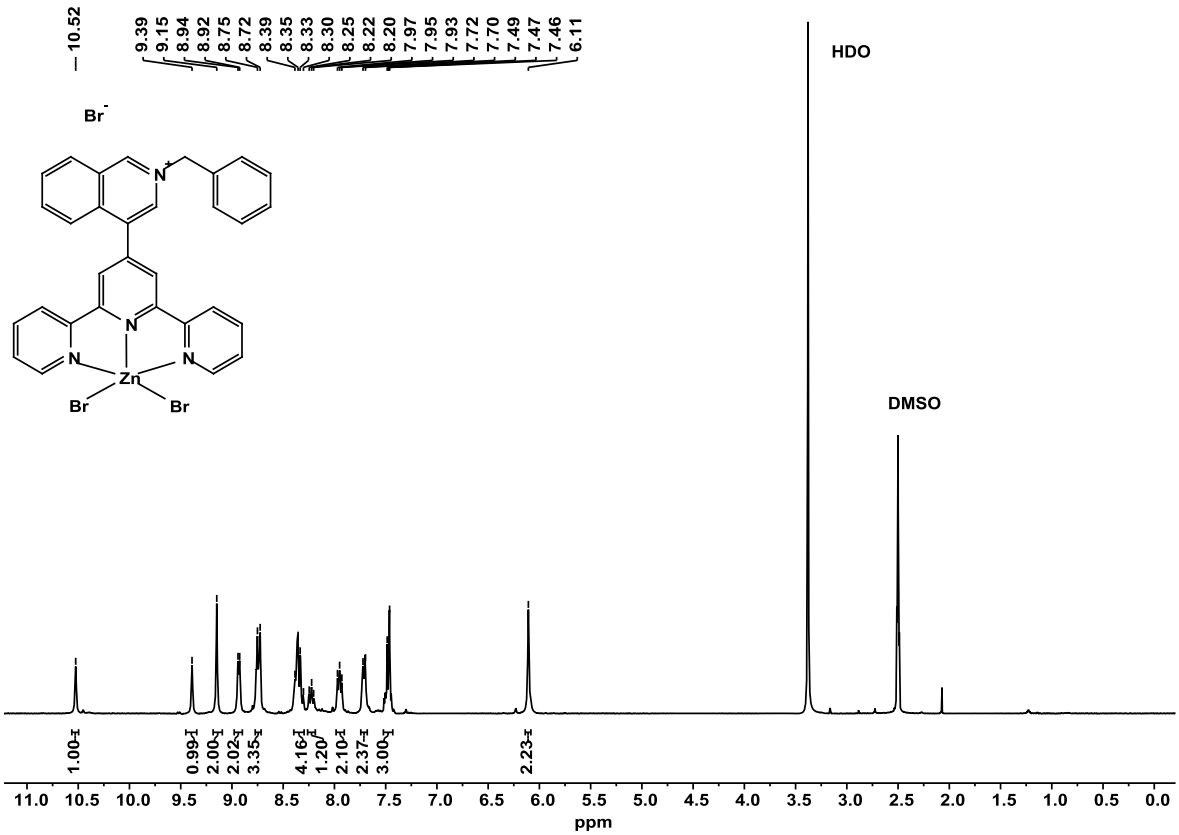

Fig. S35 ^{1}H NMR spectrum of **5.Zn** in DMSO-d_6.

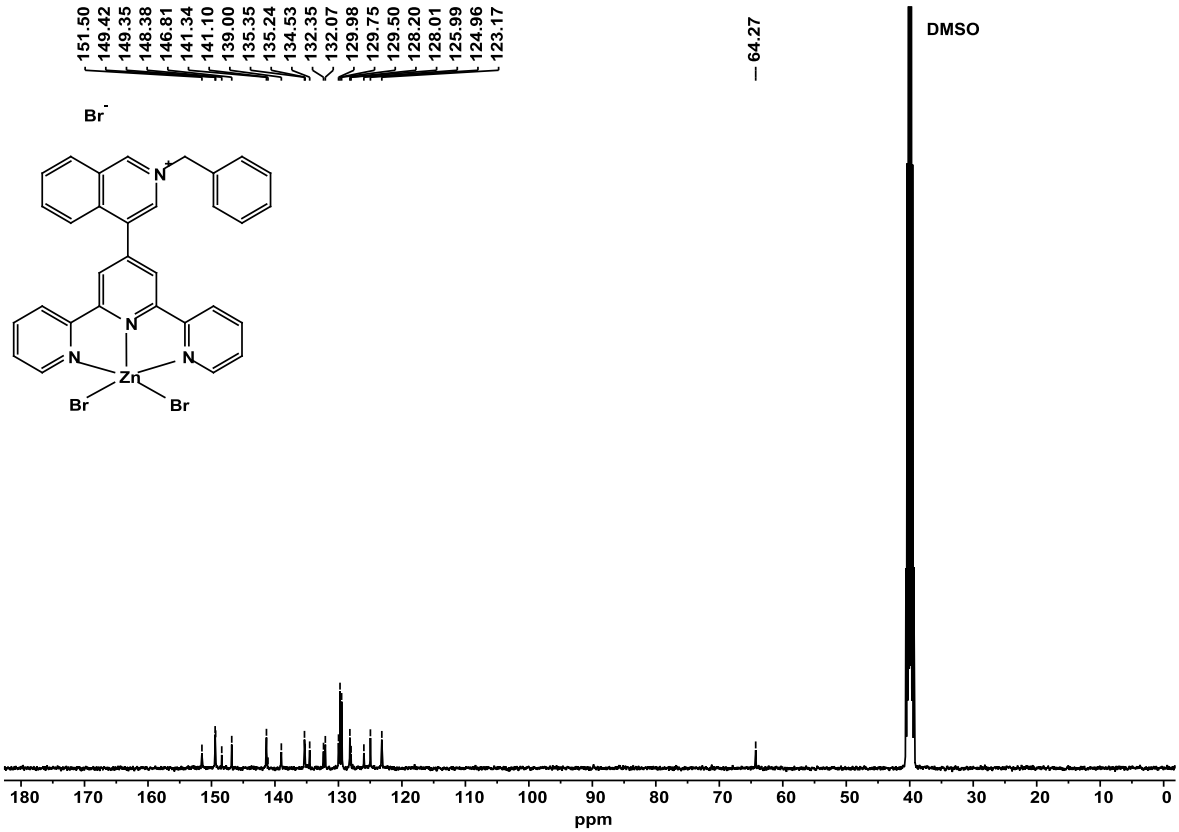

Fig. S36 ^{13}C NMR spectrum of **5.Zn** in DMSO-d_6.

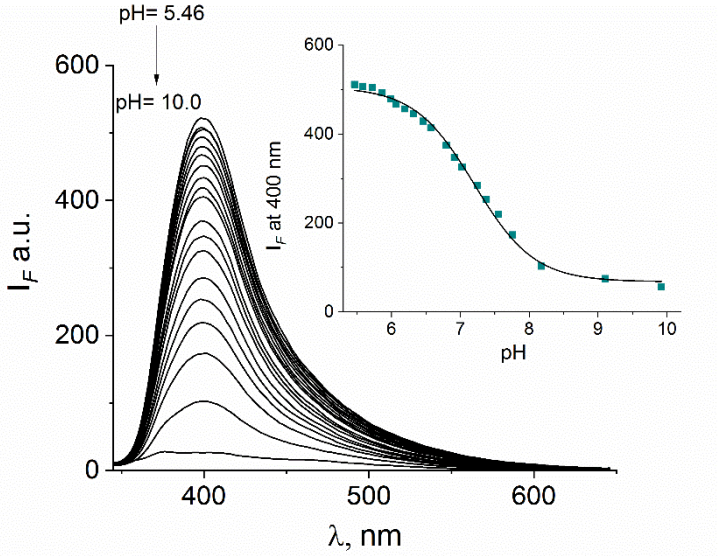

Fig. S37 Fluorescence pH-titration of buffered aqueous solution of **3.Zn** (20 μM). The inset show pH-titration profile observed at emission maxima.

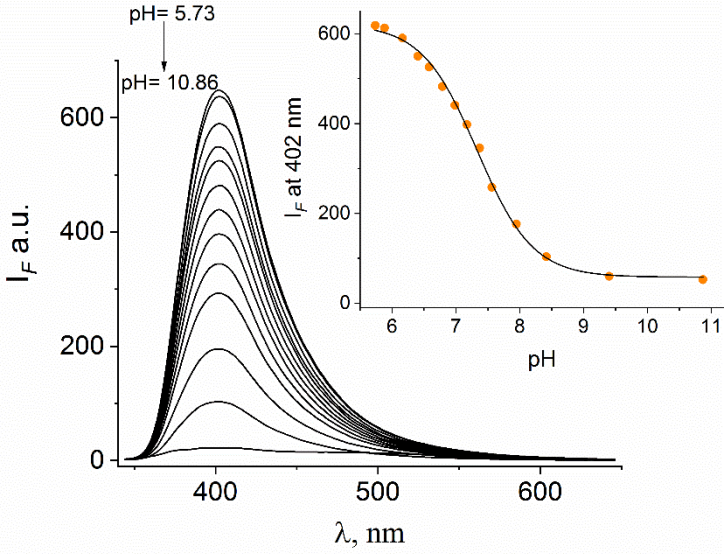

Fig. S38 Fluorescence pH-titration of buffered aqueous solution of **4.Zn** (20 μM). The inset show pH-titration profile observed at emission maxima.

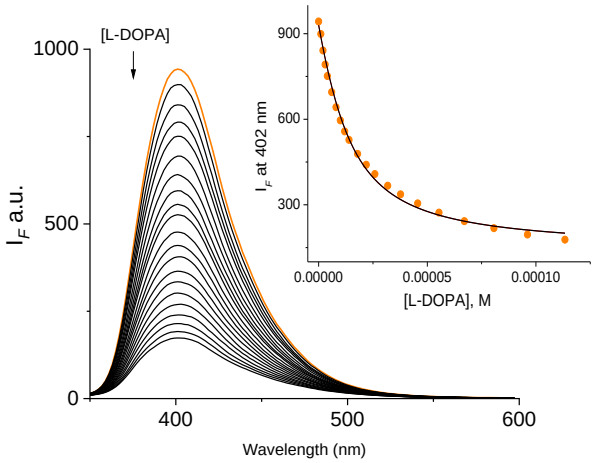

Fig. S39 Changes of emission spectra (λ_{ex} = 330 nm) of buffered aqueous solutions at pH 7.4 of **4.Zn** (10 μM) upon addition of increasing amounts of L-DOPA. The inset shows the profile at 402 nm. The solid line was obtained by fitting to Eq. (1).

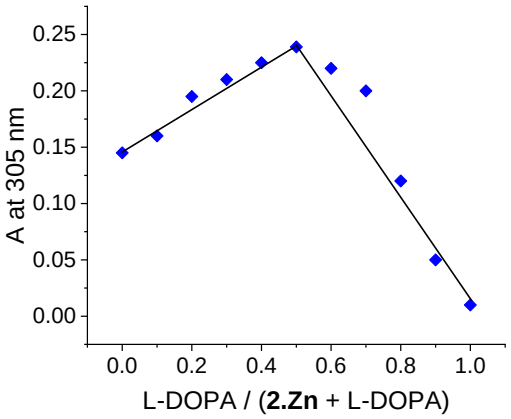

Fig. S40 Stoichiometric analysis of **2.Zn** by Job plot with L-DOPA at 305 nm

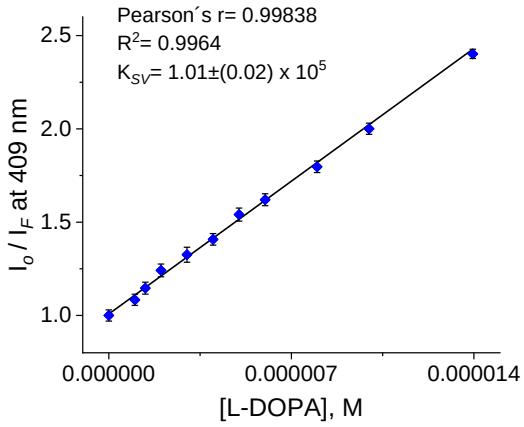

Fig. S41 Stern–Volmer plot of **2.Zn** upon addition of L-DOPA at 409 nm (λ_{ex} = 330 nm) at pH= 7.4.